

Brief communication: Nowcasting of precipitation for leading edge erosion-safe mode

Anna-Maria Tilg¹, Charlotte Bay Hasager¹, Hans-Jürgen Kirtzel², Poul Hummelshøj³

¹Department of Wind Energy, Technical University of Denmark, Roskilde, 4000, Denmark

5 ²METEK Meteorologische Messtechnik GmbH, Elmshorn, 25337, Germany

³METEK Nordic ApS, Roskilde, 4000, Denmark

Correspondence to: Anna-Maria Tilg (anmt@dtu.dk)

Abstract. Leading edge erosion (LEE) of wind turbine blades is caused by the impact of hydrometeors, which appear in solid or liquid phase. A reduction of the wind turbine blades' tip speed during defined precipitation events can mitigate LEE. To
10 apply such an erosion-safe mode, a precipitation nowcast is required. Theoretical considerations indicate that the time a
raindrop needs to fall to the ground is sufficient to reduce the tip speed. Furthermore, it is described that a compact vertical
pointing radar that measures rain in different heights with a sufficient high spatio-temporal resolution can nowcast rain for an
erosion-safe mode.

1 Introduction

15 Leading edge erosion caused by precipitation impinging on blades with high tip speed results in rougher blades and a loss in
annual energy production. According to Chen et al. (2019), the most expensive and most time-consuming process within
maintenance of wind turbines is blade repair. Durable leading edge coatings are not yet available (Herring et al., 2019).

Bech et al. (2018) propose to reduce the tip speed during severe precipitation events to limit erosion and to extend blade
20 lifetime. For example, they investigate the influence of turbine control during intense rain events on the annual energy
production (AEP). Based on some assumptions, e.g. the precipitation climate, they find that AEP increases when reducing the
tip speed during intense rain events compared to no reduction. The suggested turbine control combines wind and precipitation
measurements with a damage model. The damage model itself describes the erosion rate in relation to rain parameters (e.g.
kinetic energy or accumulated amount of rain) and is based on laboratory measurements. Hasager et al. (2020) find higher
25 erosion rates at coastal stations than inland stations in Denmark due to more intense rain events at high wind speeds at these
locations. Furthermore, they show an increase in the profit reducing the tip speed to 60 m/s or lower in case the rain intensity
exceeds 1 mm/h.

The method of erosion-safe mode control is only possible to implement based on adequate precipitation nowcasting at minute
30 to second scale. To limit the power production loss it is important to reduce the tip speed as early as possible, as long as needed
and as short as possible.

Nowcasting of rain characteristics for leading edge erosion-safe mode control based on radar and Doppler lidar is a brand new
topic in wind energy. The proposed precipitation nowcasting for erosion-safe mode has similarity to short-term forecasting for
35 power production based on ground-based remote sensing technologies like dual-Doppler radar (Valdecabres et al., 2018a) and
long-range scanning lidar at the minute scale (Valdecabres et al., 2018b). Also lidar-assisted yaw control, wake steering and
induction control at the minute to second scale observed from turbine-mounted lidars (Würth et al., 2019) are comparable to
precipitation nowcasting.

40 Radars are traditional instruments for precipitation observations while coherent Doppler lidar is novel in relation to rain (Aoki
et al., 2016; Sjöholm and Mikkelsen, 2018). This brief communication focuses on the radar-based precipitation nowcasting for
erosion-safe mode.

2 Theory

The time until a hydrometeor hits the ground is governed by three parameters: distance between cloud base height and the
45 ground and the type and size of the hydrometeor, which determine the resulting fall velocity.

The distance between the cloud base height and the ground depends mainly on the location, the storm type and the related
cloud type. It can vary between a few hundreds to some thousands of meters. Depending on the storm type and the related
growth mechanisms of cloud droplets, hydrometeors falling out of the cloud are liquid (drizzle, rain) or solid (snow, graupel,
50 hail). Solid hydrometeors start to melt when they pass the 0°C isotherm, which is the upper boundary of the melting layer. In
weather radar measurements this layer is identified by high reflectivity values and is therefore called bright band. Thurai and
Iguchi (2000) present a seasonal- and latitude-dependent distribution of the bright band height for stratiform events based on
satellite measurements where the bright band height is the height with the highest reflectivity value. They find large seasonal
variations of the bright band height for higher latitudes. Furthermore, they show that the 0°C isotherm from Recommendation
55 ITU-R P.839-1 is usually 500 m or less above the bright band height. According to an updated version, P.839-4, the mean
annual 0°C isotherm is around 2000 m above sea level for Denmark (International Telecommunication Union, 2013). This
distance leads to a bright band height of about 1500 m, which can be taken as a rough approximation for the distance a raindrop
falls until it reaches the ground. The bright band height in Denmark varies from about 3500 m in summer to 0 m in winter
(Rashpal S. Gill, Danish Meteorological Institute, personal communication).

60

Rain consists of different raindrop sizes due to collision-induced breakup and coalescence of raindrops. Raindrops have diameters up to 8 mm, although raindrops with 10 mm have been observed in tropical areas (Jones et al., 2010). Small drops up to around 1 mm are spherical, while larger drops have the shape of a flattened sphere. Bringi et al. (2003) compare raindrop size distributions (DSD) from different climates. They find for convective storm types a mass-weighted mean diameter (D_m) between 1.50-1.75 mm for maritime-like environments and slightly larger D_m between 2.00-2.75 mm for continental-like environments. For stratiform storms they report D_m values between 1.25 and 1.75 mm but no clear distinction between different environments. These D_m variations show that beside location dependent influences, raindrop formation processes related to specific storm types play a major role in determining the DSD.

70 Beside its shape, the fall velocity of a hydrometeor is controlled by three forces: gravity, buoyancy and the aerodynamic drag force. The fall velocity of a raindrop in still air, called terminal fall velocity, increases with the drop diameter. This increase is linear for small sizes and non-linear for large sizes. One of the most used empiric equations to calculate the fall velocity of raindrops is based on investigations from Atlas et al. (1973) . However, this equation does not take into account the altitude dependence of the fall speed due to the reduced aerodynamic drag force with decreasing air density with increasing altitude.

75 Jones et al. (2010) provide an equation considering a density ratio factor compared to the standard atmosphere to consider this altitude dependent change. Raindrops might not achieve terminal fall velocity during (heavy) rain, because the collision-induced breakup and coalescence of drops causes repetitive increase and decrease of the fall velocity (Jones et al., 2010). Furthermore, as rain consists of different drop sizes, there will be always raindrops that are faster and slower.

80 Assuming a raindrop with a diameter of 1.5 mm, its terminal velocity is around 5 m/s taking the equation of Atlas et al. (1973). Considering a rain height of 1500 m, the raindrop needs 300 s (5 min) to fall to the ground. This time can be used to decelerate the tip speed of the wind turbine blades to reduce the impact energy by the drop and therefore the erosion of the leading edges.

Solid hydrometeors have different properties than raindrops. This difference results in different fall properties and impact behaviours on the leading edge of the wind turbine blade. The impact of hail and graupel causes more damage compared to rain. The focus of this publication is on the nowcasting of rain, as hail and graupel are less frequent (Macdonald et al., 2016) and snow is not relevant.

3 Application

Operational nowcasting provided by national weather services, like Integrated Nowcasting through Comprehensive Analysis (Haiden et al., 2011), combines available observations from weather stations, weather radars and satellites with forecasts of numerical weather prediction models. They provide values of precipitation amount and type beside other parameters in real time. However, in offshore environments, where enhanced leading edge erosion is observed, observations from weather

stations are usually not available. Furthermore, the use of C- and S-band based weather radars, which are usually installed onshore, includes some limitations, e.g. precipitation does not fill completely the scanned volume, height of radar beam is above precipitation and reflections caused by the wind farm infrastructure wrongly indicate precipitation. These limitations can be corrected only to some extent and lead to some uncertainty in the precipitation parameters. Local installed sensors measuring vertical profiles of precipitation are therefore an interesting option for nowcasting using the described time difference between the detection and impact of raindrops. Takahashi (1990) presents the Precipitation Particle Image Sensor (PPIS). This sensor measures like a radiosonde the precipitation at a certain height while ascending through the atmosphere. In contrast, vertical pointing radars provide continuous precipitation measurements in different altitudes at the same time.

An example for a ground-based vertical pointing radar is the Micro Rain Radar (MRR) from METEK. It is a compact 24 GHz (K-band) frequency modulated continuous wave (FM-CW) Doppler radar with a parabola antenna pointing vertically (Peters et al., 2002). The latest model MRR-PRO has a vertical resolution of > 10 m and can provide an averaged Doppler spectrum of the hydrometeors in ≥ 1 s, i.e. a Doppler spectrum roughly each 10 m for each second is available.

In case of rain, the first moment of the measured Doppler spectra allows the estimation of the fall velocity of the raindrops via the Doppler velocity. Based on the calculated fall velocity, the raindrop size can be estimated using the previously mentioned relation between these two parameters inversely. The availability of the raindrop size and fall velocity allows the calculation of further rain parameters like the rain reflectivity and rain intensity (assuming Rayleigh approximation) for different heights. These calculations assume that only raindrops and no solid hydrometeors or mix of both (i.e. sleet) backscatter the signal.

Figure 1 shows the temporal and vertical evolution of the radar reflectivity, fall velocity and rain intensity of an event in December 2019 in Plymouth (United Kingdom) measured with a MRR-PRO. This MRR-PRO provided data every 10 s up to 3200 m above ground. The high values of the derived parameters reflectivity and rain intensity between 2000 m and 1600 m indicate a melting layer. Below this layer, precipitation falls as rain, where rain intensity close to the ground is above 5 mm/h for several consecutive minutes. Rain that was registered at the lower boundary of the melting layer for example at 17:34 arrived around 2 min later at turbine hub height (approximately 100 m above ground). This time difference is shorter than the expected time based on the above calculations. One reason is the reduced air density and therefore reduced aerodynamic drag in higher altitudes that leads to a higher fall velocities. Additionally, because of break-up and coalescence processes, the actual fall velocity can differ from the terminal fall velocity with velocities even above terminal fall velocity (Montero-Martínez et al., 2009). Nevertheless, in principle the measured time difference would enable the erosion-safe mode control to reduce the tip speed of the wind turbine blades in due time. Based on the results from Hasager et al. (2020) one can assume that at this rain intensity the tip speed will be reduced around this value. Furthermore, the height information of the melting layer can also help to identify the risk of blade icing, especially in cold climates.

The calculations of the rain parameters assume still air. In stratiform rain events the vertical wind speed is quite low, whereas vertical wind speeds during convective events like thunderstorms can be high. This assumption introduces some uncertainty in the calculated rain parameters in situations with high vertical wind speeds. The MRR measurements are not disturbed by the flow around the sensor in contrast to in-situ sensors like disdrometers (Testik and Rahman, 2016).

The automatic detection of solid hydrometeors with an MRR is still challenging as these precipitation types have different fall properties than rain. However, they can be detected by the synopsis of different rain parameters provided by the MRR.

135

2019-12-13 17:00-18:00 UTC

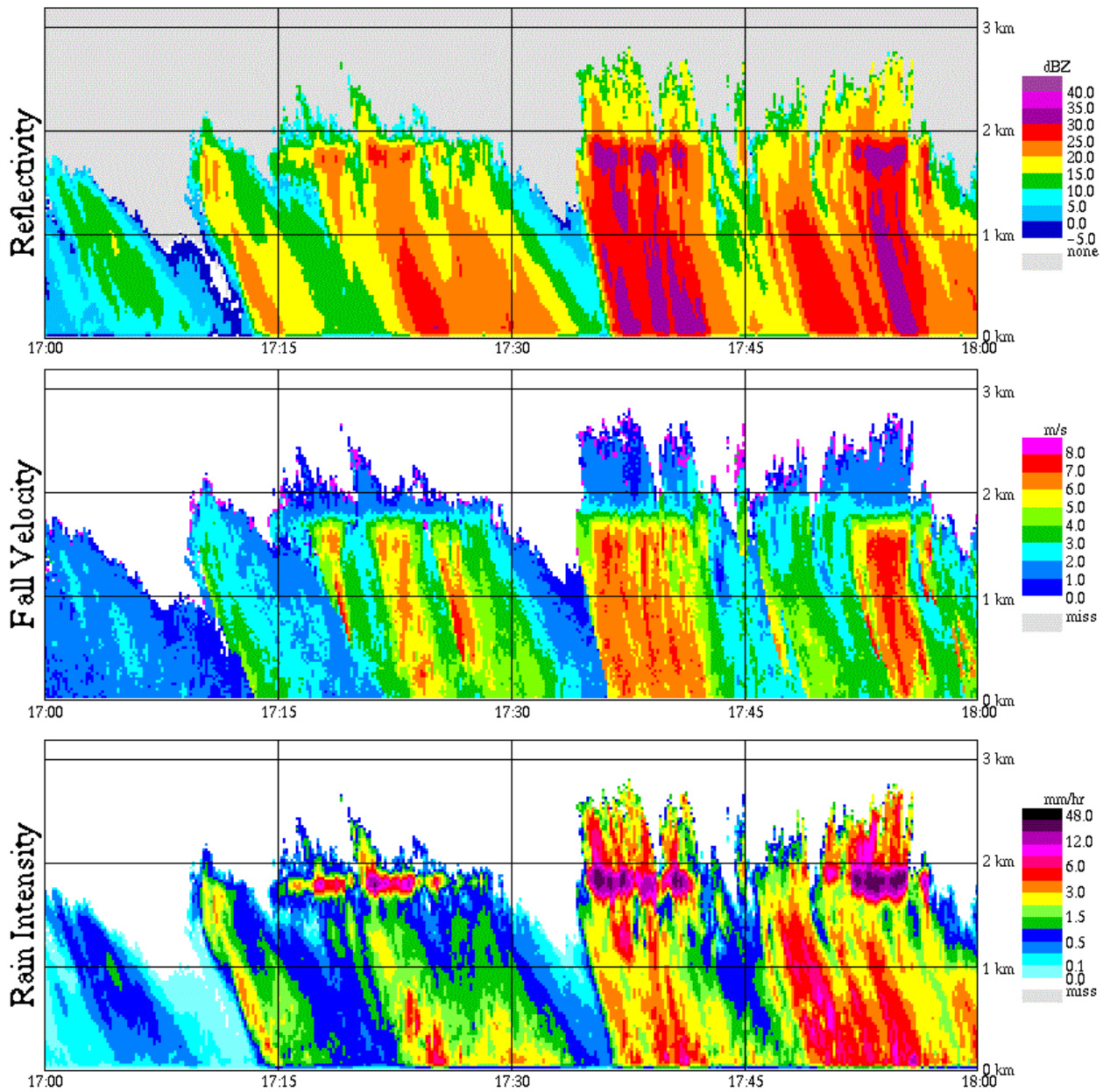


Figure 1: Radar reflectivity [dBz], fall velocity of raindrops [m/s] and rain intensity [mm/h] based on Micro Rain Radar measurements in Plymouth (United Kingdom). The vertical axis describes the vertical distance from the sensor and the horizontal axis the time in UTC.

4 Conclusion

Erosion-safe mode needs, like other parameters in wind turbine controlling, a nowcasting with high temporal and spatial resolution. Theoretical investigations showed that it takes a raindrop around five minutes (or less) to cover the distance between the cloud and the ground. If the raindrop is detected when it starts to fall, this time difference is sufficient to enable erosion-safe mode with reduced tip speed. Vertical precipitation profiles can be obtained using vertical pointing radars. For example, the Micro Rain Radar (MRR) from METEK points strictly vertically and measures Doppler spectra up to three kilometres with a resolution > 10 m. Due to the high temporal resolution, the Doppler spectra and the related rain parameters are updated frequently and can be used for nowcasting. Using a vertical pointing radar also allows capturing the height and temporal evolution of a possible present melting layer and solid hydrometeors. Based on these reflections it is possible to measure and nowcast rain where vertical precipitation profiles with a high spatio-temporal resolution are essential. This nowcasting technique can be applied onshore and offshore. Future work includes the combination of vertical pointing radar measurements and damage models to improve erosion-safe mode models and their operational use.

Author contribution

A.-M. Tilg: developed and discussed the concept, wrote main parts of the text. **C. Hasager:** discussed concept, wrote and edited text. **H.-J. Kirtzel:** discussed the concept, edited text. **P. Hummelshøj:** discussed the concept, edited text.

Competing interests

The author **H.-J. Kirtzel** is employed by the private company METEK GmbH and author **P. Hummelshøj** is employed by the private company METEK Nordic ApS. The companies develop, produce and sell the Micro Rain Radar (MRR). The authors declare that they have no other known competing financial interests or personal relationships that could have appeared to influence the work reported in this paper.

Acknowledgements

We thank Chris Kidd (University of Maryland, NASA) for providing us the measurement example of the Micro Rain Radar installed at the Plymouth Marine Laboratory where Tim Smyth is responsible for the observations. This work was supported by the Innovation Fund Denmark grant 6154-00018B for the project EROSION (<http://www.rain-erosion.dk>; last access 13 January 2020). We thank two anonymous reviewers for their comments.

References

- Aoki, M., Iwai, H., Nakagawa, K., Ishii, S. and Mizutani, K.: Measurements of Rainfall Velocity and Raindrop Size Distribution Using Coherent Doppler Lidar, *J. Atmos. Oceanic Technol.*, 33(9), 1949–1966, doi:10.1175/JTECH-D-15-0111.1, 2016.
- 170 Atlas, D., Srivastava, R. C. and Sekhon, R. S.: Doppler radar characteristics of precipitation at vertical incidence, *Rev. Geophys.*, 11(1), 1–35, doi:10.1029/RG011i001p00001, 1973.
- Bech, J. I., Hasager, C. B. and Bak, C.: Extending the life of wind turbine blade leading edges by reducing the tip speed during extreme precipitation events, *Wind Energ. Sci.*, 3(2), 729–748, doi:10.5194/wes-3-729-2018, 2018.
- 175 Bringi, V. N., Chandrasekar, V., Hubbert, J., Gorgucci, E., Randeu, W. L. and Schoenhuber, M.: Raindrop Size Distribution in Different Climatic Regimes from Disdrometer and Dual-Polarized Radar Analysis, *J. Atmos. Sci.*, 60(2), 354–365, doi:https://doi.org/10.1175/1520-0469(2003)060%3C0354:RSDIDC%3E2.0.CO;2, 2003.
- Chen, J., Wang, J. and Ni, A.: A review on rain erosion protection of wind turbine blades, *J Coat Technol Res*, 16(1), 15–24, doi:10.1007/s11998-018-0134-8, 2019.
- 180 Haiden, T., Kann, A., Wittmann, C., Pistotnik, G., Bica, B. and Gruber, C.: The Integrated Nowcasting through Comprehensive Analysis (INCA) System and Its Validation over the Eastern Alpine Region, *Wea. Forecasting*, 26(2), 166–183, doi:10.1175/2010WAF2222451.1, 2011.
- Hasager, C., Vejen, F., Bech, J. I., Skrzypiński, W. R., Tilg, A.-M. and Nielsen, M.: Assessment of the rain and wind climate with focus on wind turbine blade leading edge erosion rate and expected lifetime in Danish Seas, *Renewable Energy*, 149, 91–102, doi:10.1016/j.renene.2019.12.043, 2020.
- 185 Herring, R., Dyer, K., Martin, F. and Ward, C.: The increasing importance of leading edge erosion and a review of existing protection solutions, *Renewable and Sustainable Energy Reviews*, 115, 109382, doi:10.1016/j.rser.2019.109382, 2019.
- International Telecommunication Union: Recommendation ITU-R P.839-4 - Rain height model for prediction methods, International Telecommunication Union (ITU). [online] Available from: <http://www.itu.int/pub/R-REC/en> (Accessed 9 December 2019), 2013.
- 190 Jones, B. K., Saylor, J. R. and Testik, F. Y.: Raindrop morphodynamics, in *Geophysical Monograph Series*, vol. 191, edited by F. Y. Testik and M. Gebremichael, pp. 7–28, American Geophysical Union, Washington, D. C., 2010.
- Macdonald, H., Infield, D., Nash, D. H. and Stack, M. M.: Mapping hail meteorological observations for prediction of erosion in wind turbines: UK hail meteorological observations, *Wind Energy*, 19(4), 777–784, doi:10.1002/we.1854, 2016.
- 195 Montero-Martínez, G., Kostinski, A. B., Shaw, R. A. and García-García, F.: Do all raindrops fall at terminal speed?, *Geophys. Res. Lett.*, 36(11), L11818, doi:10.1029/2008GL037111, 2009.
- Peters, G., Fischer, B. and Andersson, T.: Rain observations with a vertically looking Micro Rain Radar (MRR), *Boreal Environment Research*, 7(4), 353–362, 2002.
- Sjöholm, M. and Mikkelsen, T.: EROSION D3.1 Lidar tested versus disdrometer, Technical University of Denmark. [online] Available from: <http://www.rain-erosion.dk/publication> (Accessed 14 January 2020), 2018.

- 200 Takahashi, T.: Near absence of lightning in torrential rainfall producing Micronesian thunderstorms, *Geophys. Res. Lett.*, 17(13), 2381–2384, doi:10.1029/GL017i013p02381, 1990.
- Testik, F. Y. and Rahman, M. K.: High-Speed Optical Disdrometer for Rainfall Microphysical Observations, *J. Atmos. Oceanic Technol.*, 33(2), 231–243, doi:10.1175/JTECH-D-15-0098.1, 2016.
- 205 Thurai, M. and Iguchi, T.: Rain height information from TRMM precipitation radar, *Electronics Letter*, 36(12), 1059–1061, 2000.
- Valdecabres, L., Nygaard, N., Vera-Tudela, L., von Bremen, L. and Kühn, M.: On the Use of Dual-Doppler Radar Measurements for Very Short-Term Wind Power Forecasts, *Remote Sensing*, 10(11), 1701, doi:10.3390/rs10111701, 2018a.
- Valdecabres, L., Peña, A. and Courtney, M.: Very short-term forecast of near-coastal flow using scanning lidars, *Wind Energy Science*, 3, 313–327, doi:https://doi.org/10.5194/wes-3-313-2018, 2018b.
- 210 Würth, I., Valdecabres, L., Simon, E., Möhrlen, C., Uzunoğlu, B., Gilbert, C., Giebel, G., Schlipf, D. and Kaifel, A.: Minute-Scale Forecasting of Wind Power—Results from the Collaborative Workshop of IEA Wind Task 32 and 36, *Energies*, 12(4), 712, doi:10.3390/en12040712, 2019.